

Evaluation of Extra- and Intracellular Apparent Diffusion in Normal and Globally Ischemic Rat Brain via ^{19}F NMR

Timothy Q. Duong, Joseph J. H. Ackerman, Howard S. Ying, Jeffrey J. Neil

The biophysical mechanism(s) underlying diffusion-weighted MRI contrast following brain injury remains to be elucidated. Although it is generally accepted that water apparent diffusion coefficient (ADC) decreases after brain injury, it is unknown whether this is associated with a decrease in intracellular or extracellular water displacement, or both. To address this question, 2- ^{19}F fluoro-2-deoxyglucose-6-phosphate (2FDG-6P) was employed as a compartment-specific marker in normal and globally ischemic rat brain. Through judicious choice of routes of administration, 2FDG-6P was confined to the intra- or extracellular space. There was no statistical difference between intra- and extracellular 2FDG-6P ADCs in normal or in globally ischemic brain ($P > 0.16$), suggesting that water ADCs in both compartments are similar. However, ischemia did result in a 40% ADC decrease in both compartments ($P < 0.001$). Assuming that 2FDG-6P reflects water motion, this study shows that water ADC decreases in both spaces after ischemia, with the reduction of intracellular water motion being the primary source of diffusion-weighted contrast.

Key words: apparent diffusion coefficient; ADC; stroke; deoxyglucose-6-phosphate; DWI.

INTRODUCTION

Diffusion-weighted magnetic resonance imaging (DWI), in which contrast is based on water apparent diffusion coefficient (ADC), is widely recognized as a useful imaging modality because of its ability to detect central nervous system (CNS) injury within minutes after its onset, whereas other conventional imaging techniques (such as T_2 -, T_1 -, ρ -weighted MRI and CT) fail to detect such injury for at least a few hours (1–4). The ADC value of water in brain decreases rapidly after many forms of CNS injury, including stroke (4, 5), trauma (6), status epilepticus (7–10), excitotoxic injury (11, 12), and spreading depression (13–16). As a result, DWI is a potentially

useful diagnostic tool for early detection and quantitative identification of CNS injury as well as assessment of therapeutic response. Despite this considerable clinical potential, the biophysical mechanism(s) leading to diffusion-weighted MRI contrast remains poorly understood.

In MRI, the smallest common volume element, typically a voxel with a volume of few μl , encompasses millions of cells. Under most conditions, the measured ADC values reflect a combination of ADC values in both the extra- and intracellular compartments within the voxel. Further, it is generally believed that the ADC of water in the intracellular space is less than that of water in the extracellular space (4, 9, 12). Based on these considerations, several mechanisms have been postulated to explain the decrease in ADC following CNS injury, namely: (i) cell swelling associated with CNS injury, causing a net migration of more rapidly diffusing extracellular water into the more slowly diffusing intracellular space (4, 5, 9, 12, 17); (ii) reduction of intracellular water ADC due to a loss of cytoplasmic motion and/or an increase in viscosity of intracellular milieu (9, 18–20); (iii) reduction in extracellular water ADC due to increased restriction to diffusion in the extracellular space because of cell swelling and loss of extracellular volume (21–24); and (iv) reduction in transmembrane water movement (25).

The hypotheses listed above are rational yet exceedingly difficult to validate due to the complex nature of the biological system under investigation. The CNS is a multicompartment system, presumably with different ADC values in different compartments, restriction of diffusion within compartments, and exchange of water between compartments. After neuronal cell injury, any or all of these factors, including compartment size, may change and affect the overall brain tissue water ADC values. Furthermore, the proposed mechanisms described above are not necessarily mutually exclusive and may depend on the model of cell injury. Defining which mechanism(s) plays a role in DWI contrast may lead to a better quantification of cell injury (perhaps salvageable versus nonsalvageable) and to an improvement in experimental design. This would lay the groundwork for more effective use of this powerful imaging modality in clinical as well as research settings.

We suggest that the first step in investigating such a complex multicompartment system is to determine what happens to ADC values in each compartment in the face of cell injury—ideally, independent or cognizant of water exchange between compartments. As part of a continuing effort, we present herein the use of 2- ^{19}F fluoro-2-deoxyglucose-6-phosphate (2FDG-6P) as a compartment-spe-

MRM 40:1–13 (1998)

From the Department of Chemistry (T.Q.D., J.J.H.A.), Washington University, St. Louis, Missouri; Departments of Radiology and Internal Medicine (J.J.H.A.), and Department of Neurology (H.S.Y.), Washington University School of Medicine, St. Louis, Missouri; and Department of Neurology (J.J.N.), Division of Pediatric Neurology, St. Louis Children's Hospital, St. Louis, Missouri.

Address correspondence to: Jeffrey J. Neil, MD, PhD, Pediatric Neurology, St. Louis Children's Hospital, One Children's Place, St. Louis, MO 63110. Received November 26, 1997; revised February 23, 1998; accepted February 23, 1998.

This research was supported in part by a grant from the McDonnell Center for Higher Brain Function, NIH grant NS35912, and a Graduate Student Training Grant (GAANN, P200A40147–96) from the Department of Education.

1998 ISMRM Young Investigators' Rabi Award Winner.

0740-3194/98 \$3.00

Copyright © 1998 by Williams & Wilkins

All rights of reproduction in any form reserved.

cific marker to report on the extra- and intracellular ADCs in normal and globally ischemic rat brain via ^{19}F MR diffusion spectroscopy. Localization of 2FDG-6P to the extracellular space results when it is administered directly via intracerebroventricular infusion. The same molecule can be confined to the intracellular space when its nonphosphorylated metabolic precursor, 2- ^{19}F fluoro-2-deoxyglucose (2FDG), is administered via intravenous infusion (26, 27). In addition to these *in situ* rat brain experiments, neuronal tissue culture experiments were performed to confirm the extra- and intracellular compartment specificity of 2FDG-6P under normal and ischemic conditions.

Although it is clear that the diffusion of 2FDG-6P is not the same as that of water in biological tissues, it is likely that changes in ADCs of compartment-specific 2FDG-6P reflect similar changes in ADC of compartment-specific water in the absence of transmembrane exchange (*vide infra*). Thus, compartment-specific changes in ADCs of water can be inferred from these measurements.

MATERIALS AND METHODS

Phantom Experiment

Experiments with test (phantom) samples were performed to verify that the diffusion coefficient of 2FDG-6P (molecular weight (MW) = 260) changes in parallel with that of water. In these experiments, 2.5 mg of 2FDG-6P (D & J Scientific) were dissolved in 0.5 ml of 0.9% saline or 20% bovine serum albumin (BSA) gel. The diffusion coefficients in aqueous and gel phantoms were measured using the Stejskal-Tanner diffusion sequence (28) with eight b values ranging from 0 to 3000 s/mm^2 and $4 \cdot T_1$ delay between acquisitions. The other diffusion measurement sequence parameters were $\text{TE} = 43$ ms, $\Delta = 26.4$ ms, $\delta = 12.5$ ms, and diffusion time $t_{\text{diff}} = 22.2$ ms (see Eq. [1b] for definitions). Longitudinal relaxation time constants (T_1 s) were measured using the conventional [delay- 180° - τ - 90° -acquire] inversion-recovery pulse sequence (29, 30) with seven inversion delays (τ) and a delay of $\sim 5 \cdot T_1$ between acquisitions. Transverse relaxation time constants (T_2 s) were measured using the Carr-Purcell (Hahn) conventional [delay- 90° -TE/2- 180° -TE/2-acquire] spin-echo pulse sequence (31, 32) with six TE values and a delay of $\sim 4 \cdot T_1$ between acquisitions.

In Vitro Neuronal Tissue Culture

Tissue Culture Preparation

Tissue culture experiments were performed to evaluate the extra- and intracellular compartment specificity of 2FDG-6P. A general description of the tissue culture protocol used here can be found elsewhere (33, 34). Briefly, mixed neocortical cultures containing both neurons and glia were prepared from fetal mice at 14–17 days gestation. Approximately 1.5×10^6 cells per culture well were plated in the presence of nutrient medium containing Eagle's minimal essential medium (Earle's salts, supplied glutamine-free, from Sigma), 10 mM glucose, 2 mM glutamine, and 10% horse serum. Cultures were maintained at 37°C in a humidified incubator containing 5% CO_2 and atmospheric O_2 . Cell cultures were used for experi-

ment between 14 and 16 days after plating. All experiments were performed in quadruplicate.

2FDG-6P as an Intracellular Compartment-Specific Marker

Experiments were performed to assess the intracellular compartment specificity of 2FDG-6P under normal and cell-injured conditions. Cells were incubated for 1 h in 400 μl of nutrient medium in the presence of 20 mM 2FDG for loading. The cells take up and convert 2FDG into 2FDG-6P that is then trapped intracellularly (27). To mimic the ischemic condition *in vivo*, cultured cells were exposed to oxygen-glucose deprivation (OGD) *in vitro*. First, the culture medium was replaced by thorough exchange with deoxygenated, glucose-free, 2FDG-free medium containing Earle's balanced salts. Cultures were then placed in a humidified 37°C incubator within an anaerobic chamber (Forma Scientific) containing a gas mixture of 5% CO_2 , 10% H_2 , and 85% N_2 for 1 or 2 h (lethal injury). As a control experiment, other cells were incubated in the oxygen deprivation (OD) chamber without glucose deprivation (i.e., with 10 mM glucose). Under these experimental conditions, oxygen deprivation alone does not induce cell injury; both oxygen and glucose deprivation *in vitro* are necessary to mimic the effects of ischemic conditions *in vivo* (33).

2FDG-6P as an Extracellular Compartment-Specific Marker

Experiments similar in concept were performed to assess the extracellular compartment specificity of 2FDG-6P under normal and cell-injured conditions. Cells were incubated for 4 h in 400 μl of nutrient medium in the presence of 2 or 20 mM 2FDG-6P (not 2FDG). First, the culture medium was replaced by thorough exchange with deoxygenated, glucose-free balanced salts containing 20 mM 2FDG-6P (for OGD condition) or, alternatively, with an addition of 10 mM glucose (for OD condition). The cells were then incubated under OD or OGD conditions for 1 or 2 h as described above. For the experiment in which 2FDG-6P is added to the extracellular space, cells were exposed to 2FDG-6P, even during oxygen deprivation.

Control Tissue Culture Experiments

As further control experiments, some cells were harvested immediately after 1 h of 2FDG intracellular loading or 4 h of 2FDG-6P extracellular exposure without OD or OGD treatment. In addition, to determine the extent of nonspecific binding of 2FDG or 2FDG-6P to the plasma membrane, cells were exposed to 20 mM of 2FDG or 2FDG-6P for 1 min, respectively.

Collection of Tissue Culture Samples

After 2FDG/2FDG-6P exposure and/or OGD/OD, the supernatant (extracellular portion) was collected. The cells were washed three times with Earle's balanced salts solution and lysed with 10 μl of 0.2% sodium dodecyl sulfate. The cell-containing lysate (intracellular portion) was then collected separately. For each well of culture

cells, 375 μl (out of 400 μl) and 200 μl (out of 210 μl) of supernatant and lysate were collected, respectively. Volumes of 40 and 50 μl of D_2O were added to supernatant and lysate, respectively, providing NMR signal for field homogeneity shimming and deuterium field/frequency lock. All samples were frozen until quantitative high-resolution ^{19}F NMR experiments could be performed.

NMR Analysis of Tissue Culture Samples

Tissue culture samples were transferred to 5-mm NMR tubes employing Shigemi inserts, yielding a volume of 240 μl . High-resolution NMR experiments were performed on an 11.75 T Varian UNITY system with a $^{19}\text{F}\{^1\text{H}\}$ Nalarac probe. ^{19}F spectra under ^1H WALTZ decoupling were obtained at 5°C using the following quantitative parameters: TR = 1.5 s, 750 transients (total acquisition time of ~20 min, including three dummy scans). Receiver frequency tuning and impedance matching, as indicated by the reflected power of the radiofrequency (RF) coils, were essentially constant for all samples. Shimming was performed on the D_2O lock signal, and ^{19}F linewidths (FWHM) of 2–3 Hz were typical of all samples. Quantification of ^{19}F signal amplitude employed an external reference signal from 40 μM 2FDG acquired under the same conditions. NMR spectra of the external reference sample were obtained at the start of, three times during, and after ^{19}F NMR examination of the numerous tissue culture samples. Two other reference samples, with concentrations of 10 and 60 μM , were used to confirm the linear relationship between concentration and ^{19}F NMR signal amplitude. With high-resolution NMR, 2FDG and 2FDG-6P ^{19}F NMR signals can be distinguished from each other via chemical shift (35–37).

In Vivo Intravenous Administration of 2FDG (2FDG-6P as an Intracellular Marker)

In this *in vivo* experiment, 2FDG-6P was used as an intracellular marker after intravenous bolus infusion of 2FDG. Seven male Sprague-Dawley rats (260–300 g) were anesthetized with 2.0–2.5% (v/v) halothane in 100% O_2 . The femoral vein was catheterized. The trachea was cannulated, and the animal was ventilated mechanically using a rodent respirator (Harvard Apparatus, Model 55–2226). A fiber-optic thermal probe (Luxtron Corp.) was inserted into the nasal cavity of the animal, and the temperature was maintained at 36–38°C throughout the MR experiment with a combination of a warm water pad and/or warm air blowing over the animal's head. Temperature monitored in this manner follows the brain temperature within 1°C (unpublished data). Part of the scalp was removed such that surface coil could be placed closer to the brain without undue RF loading. Ear and tooth bars were used to reduce motion artifact. The EKG was monitored throughout the MR experiment.

A bolus of 2FDG (500 mg/kg in 1 ml of saline solution) was administered quickly via femoral vein while the rat was inside the magnet. This dose, similar to that used by Kotyk *et al.* (38), shows no gross physiological evidence of toxicity. For each rat, three live ADC measurements were made starting 1 h after the 2FDG bolus intravenous infusion (38). The animal was then killed by pentobarbital overdose (160 mg/kg, IV) while in the magnet. ADC

measurements were continued for ~3 h after death. The temperature of the rat brain was maintained at 36–38°C, and the ventilator was left on after the death of the animal.

In Vivo Intracerebroventricular Infusion of 2FDG-6P (2FDG-6P as an Extracellular Marker)

In this *in vivo* experiment, 2FDG-6P was used as an extracellular marker via intracerebroventricular infusion of 2FDG-6P. Six male Sprague-Dawley rats (280–320 g) were anesthetized with pentobarbital (35 mg/kg, IP). The trachea was cannulated, and the animal was allowed to breath unassisted during intracerebroventricular infusion. The animal was placed in a stereotaxic head frame (Kopf, Inc.) for intracerebroventricular infusion. Two holes, 1.5 mm in diameter, were drilled into the skull to target the lateral ventricles at coordinates of ± 1.4 mm lateral to bregma, 0.9 mm posterior from bregma, and 3.5 mm deep from the dura. A total of 80 μmol of 2FDG-6P in 45 μl were infused into both lateral ventricles simultaneously via an infusion pump over 3 h. Pentobarbital anesthesia was supplemented at 6 mg/kg every half hour or when needed. After intracerebroventricular infusion and throughout the MR experiment, the anesthetized animal was mechanically ventilated with 1–2% (v/v) halothane in 100% O_2 .

For each rat, three live ADC measurements were made starting 3 h after 2FDG-6P intracerebroventricular infusion. The timing origin is taken as the middle of the 3-h infusion. This timing was chosen, based on previous experience (39), to allow the infusate to distribute uniformly throughout the interstitial space in brain. The animal was then killed, and ADC measurements continued as described above.

In Vivo MR Experiments

In vivo MR experiments employed a 4.7 T, 40-cm clear bore diameter Oxford Instruments magnet equipped with a 26-cm, 10-G/cm, actively shielded, Oxford Instruments field gradient set and a Varian UNITY INOVA console. The animal's head was placed in a laboratory-constructed transmitter/receiver set consisting of a Helmholtz transmitter (inner diameter (ID) = 12 cm) and two-turn surface coil receiver (ID = 1.7 cm) with electrical isolation greater than 40 dB between transmit and receive channels.

2FDG-6P as an Intracellular Marker

For diffusion measurements of intracellular 2FDG-6P, magnetic field shimming and anatomical multislice gradient-echo imaging were performed via $^1\text{H}_2\text{O}$ MR at 201.6 MHz with the RF coils frequency tuned and impedance matched to ^{19}F at 189.6 MHz (40). STEAM volume-localized diffusion spectroscopy was employed (41–44). A voxel of $8 \times 10 \times 10 \text{ mm}^3$ (0.8 ml) was selected from the ^1H image for ^{19}F acquisition, as shown in Fig. 1. Volume selection was used in this case to avoid possible signal contamination arising from 2FDG-6P located outside the brain when 2FDG is administered intravenously. The ^{19}F diffusion sequence parameters were TR = 840 ms, TE = 43 ms, TM = 4 ms, Δ = 28.7 ms, δ = 12.5 ms, diffusion time t_{diff} = 24.5 ms, b = 0, 2000, 4000,

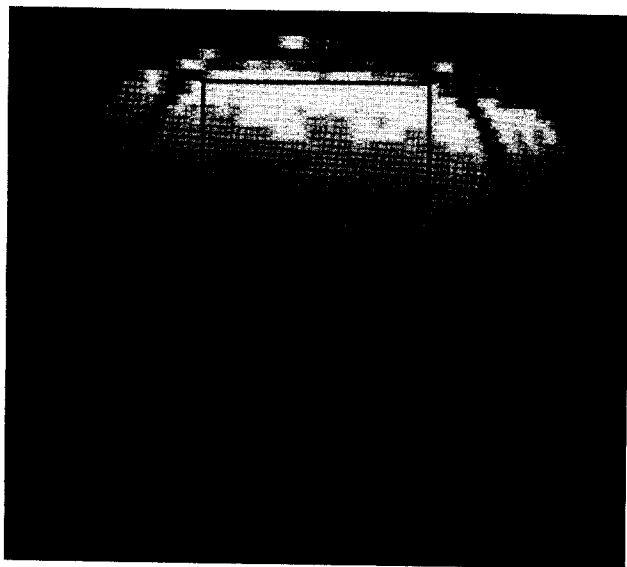


FIG. 1. A typical $^1\text{H}_2\text{O}$ anatomical (gradient-echo) image obtained with the RF coils frequency tuned and impedance matched to ^{19}F acquisition. A voxel of $8 \times 10 \times 10 \text{ mm}^3$ (0.8 ml) selected for the intracellular 2FDG-6P experiment is shown.

6000 s/mm^2 . The contribution to b values (diagonal elements of the b matrix only) due to the interactions between diffusion and nondiffusion gradients, commonly known as cross-terms, was negligible, ca. <1% as obtained from calculation and verified by phantom experiments. The number of transients was 600 or 1200, giving a temporal resolution of 30 or 60 min, respectively (three dummy scans included). Sixty min temporal resolution was initiated 1 h after the death of the animal for better signal-to-noise sensitivity, as dynamic effects were not expected. Transients were collected at four b values in an interleaved fashion to improve time course data averaging, thus reducing systematic errors that can be introduced by change in ADC values during a measurement period.

2FDG-6P as an Extracellular Marker

For diffusion measurements of extracellular 2FDG-6P, the high sensitivity of surface coil localization was used instead of STEAM volume localization because signal contamination arising from 2FDG-6P located outside the brain is not an issue (*vide infra*). The ^{19}F diffusion sequence parameters were $\text{TR} = 843 \text{ ms}$, $\text{TE} = 43 \text{ ms}$, $\Delta = 26.4 \text{ ms}$, $\delta = 12.5 \text{ ms}$, $t_{\text{diff}} = 22.2 \text{ ms}$, $b = 0, 2000, 4000, 6000 \text{ s}/\text{mm}^2$. The number of transients was 600 or 1200, which gave a temporal resolution of 30 or 60 min, respectively (three dummy scans included). Transients were collected at four b values in an interleaved fashion to reduce systematic errors. These parameters are almost identical to those used in the intracellular 2FDG-6P experiments described above so that direct comparison between the extra- and intracellular 2FDG-6P ADC values could be made. The slight difference in parameters arises from the presence of the mixing time (TM) in the STEAM volume-localized sequence used in the intracellular 2FDG-6P experiments. This introduces a difference of 2 ms in diffusion time.

Longitudinal relaxation time constants (T_1 s) of both extra- and intracellular 2FDG-6P were measured using the inversion-recovery pulse sequence described above, with seven inversion delays (τ) and a delay $\sim 4 \cdot T_1$ between acquisitions. Transverse relaxation time constants (T_2 s) were measured using the spin-echo pulse sequence described above, with four TE values and a delay of $\sim 3 \cdot T_1$ between acquisitions. T_1 and T_2 were measured with surface coil localization only to maximize signal-to-noise.

Experiments were also performed to confirm that surface coil localization leads to little signal contamination arising from 2FDG-6P located outside the brain. It is expected that when administered *via* intracerebroventricular infusion, 2FDG-6P is localized nearly exclusively to the CNS because 2FDG-6P crosses the blood brain barrier very slowly. To assess this hypothesis, 2FDG-6P was administered to three rats *via* intracerebroventricular infusion. At 3–4 h after infusion, blood (0.5 ml) was withdrawn from the femoral artery, the animal was immediately sacrificed, and cerebrospinal fluid (50–150 μl) was withdrawn from the cistern magna. Quantitative analysis employing high-resolution ^{19}F NMR was done as described. The 2FDG and 2FDG-6P concentrations in cerebrospinal fluid and blood were thus determined.

Halothane gives rise to a ^{19}F signal that is $\sim 128 \text{ ppm}$ away from the ^{19}F 2FDG-6P resonance. With the spectral width used in this study, the ^{19}F halothane resonance is strongly attenuated by the audio filters but is very weakly detectable as a double alias at 12–16 ppm upfield of the 2FDG-6P resonance.

Data Analysis

Tissue Culture Data

The ^{19}F NMR signal amplitudes were estimated using Bayesian probability theory analysis of the time domain data (45–49). The 2FDG-6P and 2FDG signals were quantified using an external reference standard, as described above. After dilution factors were taken into account and nonspecific binding of 2FDG and/or 2FDG-6P was subtracted (a minor effect), the 2FDG and 2FDG-6P concentrations in the lysate were calculated using an intracellular volume of 3.3 pl/cell and 1.5×10^6 cells/well (33). Statistical evaluation was done using analysis of variance (ANOVA).

In Vivo ^{19}F Diffusion Data

The ^{19}F signal amplitudes were estimated using Bayesian probability theory analysis of the time domain data (45–49). Amplitudes from ^{19}F diffusion data were fit to the Stejskal-Tanner equation (28) using nonlinear least square fitting to the expression,

$$S_i/S_o = \exp(-b_i \cdot \text{ADC}) \quad [1a]$$

where S_i is the signal amplitude at some value b_i , S_o is the signal amplitude with $b = 0$, and ADC is the apparent diffusion coefficient. The parameter b_i is given by

$$b_i = \gamma^2 G_i^2 \delta^2 (\Delta - \delta/3) \quad [1b]$$

where γ is the magnetogyric ratio, G_j is the gradient strength, δ is the duration of each gradient pulse, and Δ is the time between application of the two gradient pulses. $(\Delta - \delta/3)$ is also known as the diffusion time (t_{diff}) during which the ADC measurement is sensitive to motion. Statistical evaluation was done using repeated ANOVA, ANOVA, or Student's t test.

RESULTS

Phantom Experiment

The diffusion coefficients (average of two measurements) of 2FDG-6P and $^1\text{H}_2\text{O}$ in aqueous and gel phantoms at 24°C and 37°C are summarized in Table 1. The diffusion coefficients of 2FDG-6P and water change in parallel in response to viscosity and temperature variation, as expected from the Stokes-Einstein diffusion equation

$$D = kT/(6\pi\eta R_{\text{HD}}) \quad [2]$$

where k is the Boltzmann's constant, T is temperature in Kelvin, η is temperature-dependent viscosity of water, and R_{HD} is the hydrodynamic radius of the spherical particle. The degree of solvation of 2FDG-6P was briefly explored by estimating the radius of the molecule in isolation and comparing it with the hydrodynamic radius derived from MR diffusion measurements in aqueous solution via Eq. [2]. The radius of 2FDG-6P was estimated by employing the molecular modeling software INSIGHT (Molecular Simulation, CA) with the frictional coefficient of 2FDG-6P calculated for a prolate ellipsoid of revolution (50). A 2.6 Å radius was estimated for the isolated molecule, whereas the experimentally derived hydrodynamic radius was nearly twofold greater, 4.7 Å. These findings indicate that 2FDG-6P possesses an appreciable hydration shell in aqueous solution.

In Vitro Neuronal Tissue Culture

Tissue culture experiments were designed to evaluate the intra- and extracellular compartment specificity of 2FDG-6P. For the study in which 2FDG-6P was used as an intracellular marker, pharmacokinetic experiments show that optimal loading occurs with cells exposed to 2FDG for approximately 1 h (data not shown). These findings are similar to those found *in vitro* (51) and *in vivo* (38), as reported elsewhere.

The intracellular compartment trapping of 2FDG-6P was evaluated immediately after 1 h of 2FDG loading and following 1 or 2 h of OD or OGD. The intracellular 2FDG-6P concentration as determined from cell-lysate samples, ca. 650 μM , was statistically equivalent ($P > 0.3$) under all conditions (Fig. 2a). No 2FDG-6P signal was detected in the supernatant (extracellular) samples, regardless of the treatment conditions. Based on estima-

Table 1
Diffusion Coefficient ($10^{-3} \text{ mm}^2/\text{s}$) of $2\text{-}^{19}\text{F}$ FDG-6P and $^1\text{H}_2\text{O}$.

Temperature	H_2O		2FDG-6P	
	in saline	in 20% gel	in saline	in 20% gel
24°C	1.95	1.42	0.51	0.28
37°C	2.92	1.97	0.70	0.41

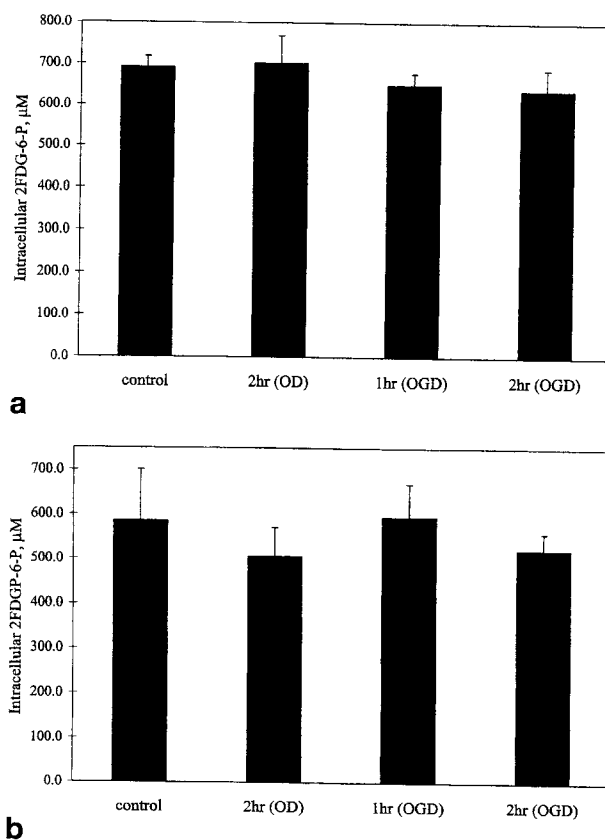


FIG. 2. (a) Intracellular concentrations of 2FDG-6P under control, oxygen deprivation (OD), and oxygen-glucose deprivation (OGD) conditions *in vitro* after 1 h of 20 mM 2FDG loading. The error bars represent the standard error of the means of four determinations. The 2FDG-6P concentrations in the lysate (intracellular portion) shown here were statistically the same ($P = 0.3$) for control, OD, and OGD conditions. In all the supernatant (extracellular portion) samples collected, no $2\text{-}^{19}\text{F}$ FDG-6P NMR signal was detected (data not shown). (b) Intracellular concentrations of 2FDG-6P under control, oxygen deprivation (OD), and oxygen-glucose deprivation (OGD) conditions *in vitro* after 4 h of 20 mM 2FDG-6P exposure. The error bars represent the standard error of the means of four determinations. The 2FDG-6P concentrations in the lysate (intracellular portion) shown here were statistically the same ($P > 0.8$) for control, OGD, and OD conditions. No 2FDG-6P was detected in lysates for 2 mM 2FDG-6P exposure. In addition, no $2\text{-}^{19}\text{F}$ FDG signal was observed in either the lysate or supernatant for either the 2 or 20 mM 2FDG-6P exposure.

tion of the MR sensitivity under these experimental settings, the limit of detectable 2FDG-6P concentration was estimated to be an intracellular concentration of $\sim 30 \mu\text{M}$. Some 2FDG (the precursor) was detected in the lysate samples and could be entirely accounted for by nonspecific binding to the plasma membrane surface (data not shown).

Similarly, the extracellular compartment specificity of 2FDG-6P was evaluated immediately after 4 h of 2FDG-6P extracellular exposure and following an additional 1 or 2 h of OD or OGD. No 2FDG-6P signal was detected in the lysate for the 2 mM 2FDG-6P extracellular exposure, regardless of the treatment conditions. For the 20 mM 2FDG-6P extracellular exposure, the intracellular 2FDG-6P concentration as determined from cell-lysate

samples (not extracellular 2FDG-6P), ca. 550 μM , was statistically equivalent ($P > 0.8$), regardless of treatment conditions (Fig. 2b). Under these conditions, there is a large 2FDG-6P concentration gradient between the extra- and intracellular space (36:1). This corresponds to <5% leakage of 2FDG-6P into the intracellular space. Using a 20:80 extracellular-to-intracellular volume ratio *in vivo*, we estimate an amplitude ratio of at least 9:1 for extracellular to intracellular 2- ^{19}F FDG-6P signals. No NMR signal arising from 2FDG (representing dephosphorylated 2FDG-6P) was detected in the lysate or the supernatant for either the 2 mM or 20 mM 2FDG-6P exposure. Nonspecific binding of 2FDG-6P to the plasma membrane surface was subtracted for the 20 mM 2FDG-6P extracellular exposure calculations. This nonspecific binding constitutes $\sim 10\%$ of the total 2FDG-6P signal before subtraction.

In Vivo Experiments

In experiments designed to confirm the CNS localization of 2FDG-6P administered via intracerebroventricular infusion, blood and cerebrospinal fluid (CSF) samples were taken 3–4 h after infusion. The 2FDG-6P concentration in CSF was $2.6 \pm 0.9 \text{ mM}$ (mean \pm SD, $n = 3$); no 2FDG was detected. No 2FDG-6P was detected in the blood plasma; however, 2FDG was found in blood at a level of ca. $0.07 \pm 0.02 \text{ mM}$ ($n = 3$). This corresponds to a factor of 37:1 in concentration of CSF 2FDG-6P to blood plasma 2FDG. This observation supports the use of high signal-sensitivity surface coil localization with little signal contamination from regions outside the brain when 2FDG-6P is administered via intracerebroventricular infusion.

The ADCs of extra- and intracellular 2FDG-6P were measured in normal and globally ischemic rat brain. Figure 3 shows representative extracellular 2FDG-6P and intracellular 2FDG-6P ^{19}F spectra. The signal amplitudes decrease with increasing b values, as expected. The signal amplitude with $b = 6000 \text{ s/mm}^2$ was attenuated to 40–50% of that with $b = 0$. Figure 4 shows a Stejskal-Tanner semilog plot of normalized signal amplitude versus b value for the data shown in Fig. 3. The data are well modeled by the Stejskal-Tanner equation (Eq. [1a]).

A summary of the rat brain ADC measurements of 2FDG-6P is graphically presented in Fig. 5. Three ADC measurements were made for each live rat, as shown by the first three data points in Fig. 5 (before and at time zero). There was no statistically significant difference between the extra- and intracellular 2FDG-6P ADC values at a given time point for normal or for globally ischemic rat brain ($P > 0.16$). However, both extracellular 2FDG-6P and intracellular 2FDG-6P ADC values fell within 30 min after the death of the animal ($P < 0.001$) and remained at a value roughly 35–40% below those obtained from the live animal. There is no statistically significant difference among the 2FDG-6P ADC values after death ($P > 0.4$ for all). Though 2FDG-6P ADC values in the two compartments are statistically indistinguishable at the 95% confidence limit, the ADC values of extracellular 2FDG-6P tended to be lower than those of the intracellular 2FDG-6P in the live animal and, in all but the initial time point (30 min), after the death of the

animal. The details of the results of Fig. 5 are given in Table 2. Analysis of the three repeated ADC measurements made on each live animal yields standard deviations less than $0.01 \times 10^{-3} \text{ mm}^2/\text{s}$, providing an intranimal precision of ca. 10%.

The ^{19}F relaxation time constants for extra- and intracellular 2FDG-6P, shown in Table 2, are statistically identical for both live and dead animals. Also, the T_2 relaxation time constant of intracellular 2FDG-6P is statistically identical in live and dead animals. However, the T_2 relaxation time constant of extracellular 2FDG-6P is 35% shorter after death of the animal. [This difference has no direct effect on the ADC measured because the S_i/S_o ratio of signal amplitudes is used in the ADC calculation. However, in ADC measurements, as in all spin-echo based protocols, signal contributions are weighted toward components with longer T_2 .]

DISCUSSION

2FDG-6P as a Compartment-Specific Marker

Relevant to experiments employing 2FDG-6P as an intracellular marker, it has been well documented (27, 38) that, when administered intravenously, 2FDG is taken up by cells via hexose receptors. 2FDG is then converted to 2FDG-6P by hexokinase. Since 2FDG-6P resists further enzymatic isomerization to a fructose-6-phosphate analog, it remains trapped within cells as 2FDG-6P unless dephosphorylated back to 2FDG by glucose-6-phosphatase. Glucose-6-phosphatase is essentially absent from brain (52–54), so 2FDG-6P is trapped in the intracellular space. This trapping process forms the basis for mapping local cerebral glucose utilization rates (55–58). The *in vitro* results reported herein confirm the intracellular compartment trapping of pharmacological levels (mM) of 2FDG-6P in healthy brain cells. Sokoloff *et al.* (27) and other researchers (26, 51, 59, 60) observed this trapping previously using tracer concentration levels (μM). The data presented here are also consistent with an *in vivo* ^{13}C (^1H) study by Kotyk *et al.* (38) employing [6- ^{13}C]2DG at pharmacological levels. At approximately 1 h after 2DG (500 mg/kg) intravenous bolus infusion in rats, they showed a prevalence of 2DG-6P over 2DG, with a ratio of about 9:1. Also, overall trapping kinetics were similar for pharmacological and tracer doses of 2DG in the study by Kotyk *et al.* In the present study, we showed further that 2FDG-6P, once trapped inside the cell, leaks out very slowly *in vitro*, at least for the first 2 h after lethal cell injury.

Relevant to experiments employing 2FDG-6P as an extracellular marker, we propose that when 2FDG-6P is infused directly into the lateral cerebral ventricles (intracerebroventricular infusion), it moves into the interstitial space of brain but does not readily cross cell membranes to enter the intracellular space. This is because this compound is hydrophilic and, therefore, unlikely to cross the plasma membrane directly. Further, there is no transporter or receptor to transport 2FDG-6P into brain cells. Consequently, 2FDG-6P, when administered directly into the cerebroventricular space, will primarily reside in the interstitial space. This hypothesis was tested using neuronal tissue culture. Less than 5% leakage from the extracellular to intracellular

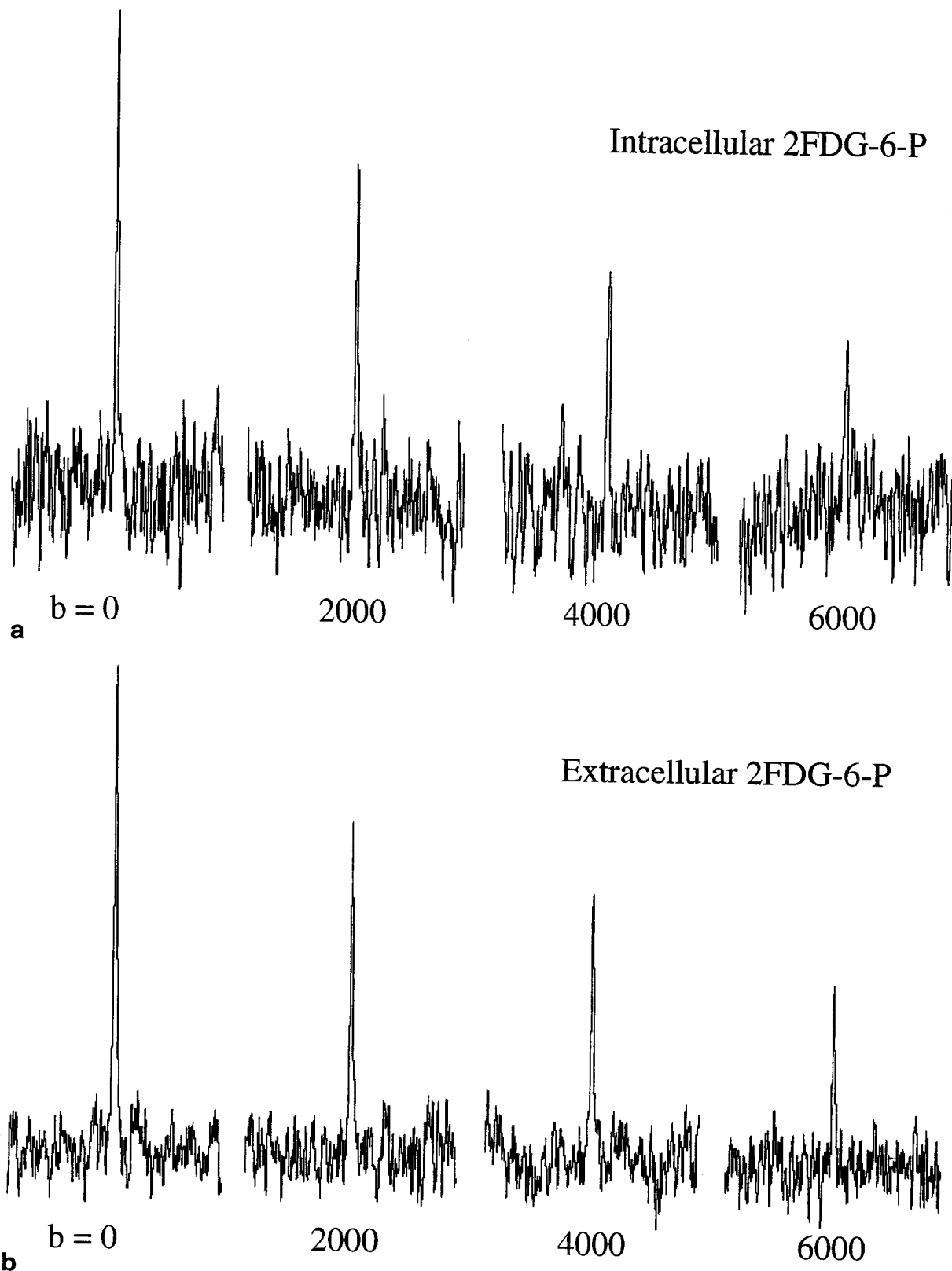


FIG. 3. (a) A series of Stejskal-Tanner diffusion ^{19}F frequency-domain spectra obtained from the brain of a live rat 1 h after intravenous infusion of 2FDG (intracellular 2FDG-6P). The spectra shown represent Fourier transform of the time-domain data after application of an exponential apodization function, resulting in a 50-Hz line broadening. The number under each spectrum represents the b value in s/mm^2 . The frequency-domain representation is used here for display purposes, but signal amplitude estimations used for data analysis were obtained using Bayesian analysis of the time-domain data as described in the text. (b) Identical to above except that these spectra are from a different rat 4 h after intracerebroventricular administration of 2FDG-6P (extracellular 2FDG-6P).

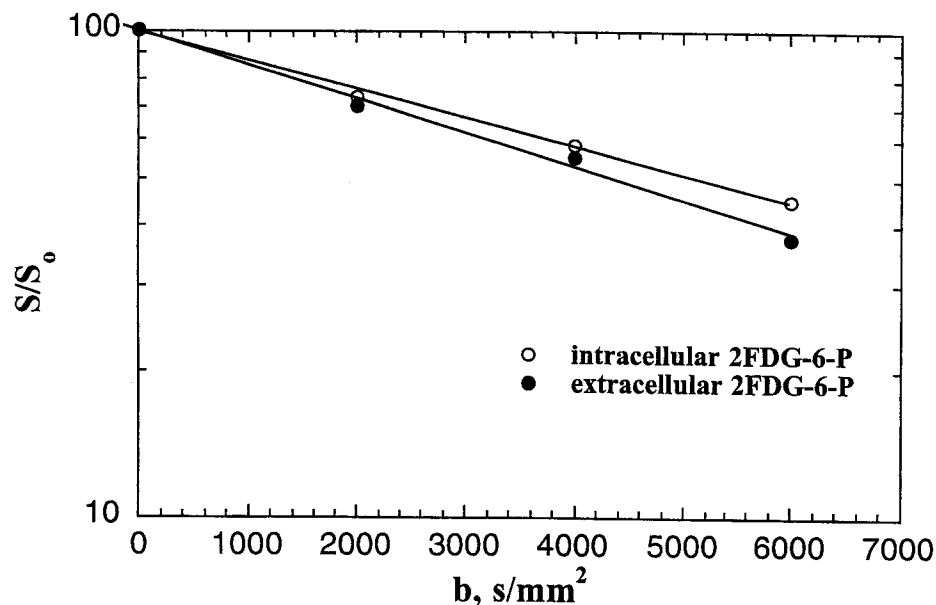


FIG. 4. A Stejskal-Tanner semilog plot of normalized signal amplitude versus b value (see Eq. [1]) corresponding to the spectral data shown in Fig. 3. The open circles indicate intracellular 2FDG-6P amplitudes, and the solid circles indicate extracellular 2FDG-6P amplitudes. The solid lines through the data points represent the nonlinear least squares fit of the data to Eq. [1].

space was observed. Based on these data, the extra- to intracellular 2- ^{19}F FDG-6P MR signal ratio was estimated to be at least 9:1 for intact rat brain. No further leakage after 2 h of lethal cell injury was observed in tissue culture. Moreover, our tissue culture results also show that 2FDG-6P added to the extracellular space was not converted back to

specific marker to reflect water motion. The diffusion coefficients of 2FDG-6P in saline and gel aqueous phantoms (Table 1) are similar to those found for other biomolecules of like size (61, 62). The diffusion coefficients of 2FDG-6P and water change in parallel and to a similar degree in response to viscosity and temperature change. Thus, the premise that changes in the motion of 2FDG-6P, as reflected via ^{19}F MR determination of ADC value, may be taken to infer parallel changes in water motion seems reasonable. When 2FDG-6P is being used as a compartment-specific probe, it is important to consider the issue of whether the compound is contained within the aqueous compartment of the cell or is bound to macromolecules. The ratio of ADC values for water and 2FDG-6P in phantom and in brain can be used to get a rough assessment of whether intracellular 2FDG-6P is bound to large macromolecules. The saline-phantom: brain ADC ratios for $^1\text{H}_2\text{O}$ (4.2) and for intracellular 2FDG-6P (5.3) are quite similar, suggesting that 2FDG-6P is unlikely to be bound. Thus, the ADC value of the intracellular 2FDG-6P is likely to be reflective of motion in the aqueous

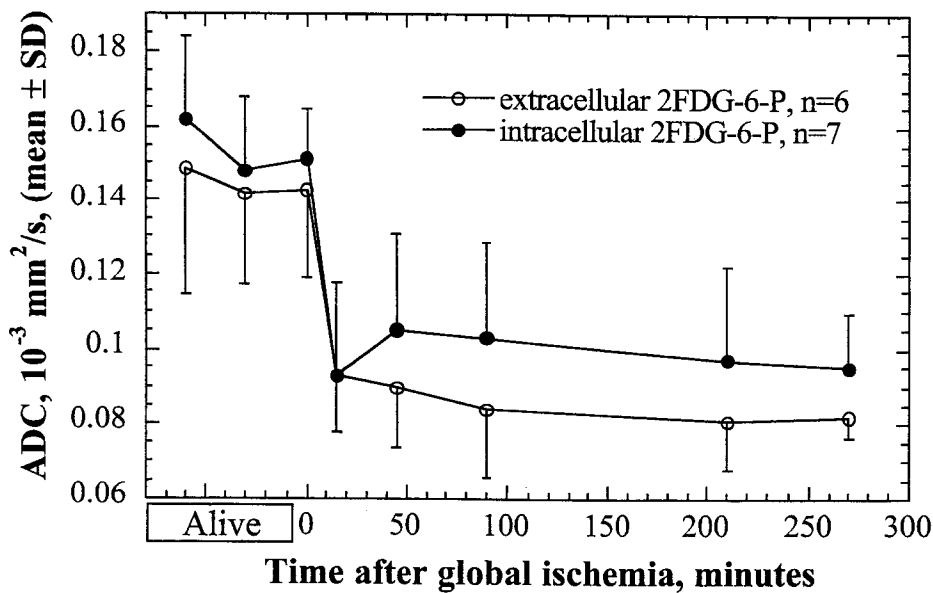


FIG. 5. A plot of intracellular (open circle) and extracellular (solid circle) 2FDG-6P ADC versus time immediately before and nearly 5 h after the death of the animals. The data points assigned -60, -30, and 0 min represent measurements from live rat. Each data point is derived from spectra collected over 30 min. The error bars represent the standard deviations. The ADCs for intra- and extracellular 2FDG-6P at a given time point were not statistically different under either normal or globally ischemic conditions. The ADCs for both compartments decrease by ca. 35–40% within minutes of the death of the animals.

its precursor, 2FDG, under normal (control and OD) or cell-injured (OGD) conditions. Therefore, 2FDG-6P can be used as an extracellular marker when administered via intracerebroventricular infusion. In addition, 2FDG-6P does not cross the blood brain barrier readily. Our analysis of blood and CSF samples shows that the intracerebroventricularly infused 2FDG-6P is highly localized to the CNS. This trapping of 2FDG-6P in the CNS also prevents loss of signal-to-noise sensitivity over the duration of the full set of ADC measurements. Furthermore, the compartmental localization permits the use of high signal-sensitivity surface-coil localization and detection with little signal contamination arising from 2FDG-6P located outside the brain.

We propose herein the use of 2FDG-6P as a compartment-specific marker to reflect water motion. The diffusion coefficients of 2FDG-6P in saline and gel aqueous phantoms (Table 1) are similar to those found for other biomolecules of like size (61, 62). The diffusion coefficients of 2FDG-6P and water change in parallel and to a similar degree in response to viscosity and temperature change. Thus, the premise that changes in the motion of 2FDG-6P, as reflected via ^{19}F MR determination of ADC value, may be taken to infer parallel changes in water motion seems reasonable. When 2FDG-6P is being used as a compartment-specific probe, it is important to consider the issue of whether the compound is contained within the aqueous compartment of the cell or is bound to macromolecules. The ratio of ADC values for water and 2FDG-6P in phantom and in brain can be used to get a rough assessment of whether intracellular 2FDG-6P is bound to large macromolecules. The saline-phantom: brain ADC ratios for $^1\text{H}_2\text{O}$ (4.2) and for intracellular 2FDG-6P (5.3) are quite similar, suggesting that 2FDG-6P is unlikely to be bound. Thus, the ADC value of the intracellular 2FDG-6P is likely to be reflective of motion in the aqueous

Table 2a
Rat Brain In Vivo Extracellular 2FDG-6P ADCs and Relaxation Time Constants at 4.7 T and 37°C (mean \pm SD, $n = 6$)

	T_1 (s)	T_2 (s)	ADC (10^{-3} mm 2 /s)
Alive	1.31 \pm 0.14	0.155 \pm 0.017	0.144 \pm 0.018
Dead	1.40 \pm 0.18	0.101 \pm 0.018	0.086 \pm 0.012 ^a

^a Average of all measurements after death.

compartment of the cell. Glucose-6-phosphate is known to be localized to the cytosol (63), and 2FDG-6P, being a glucose-6-phosphate analog, is very likely localized to the cytosol as well. Water is present in both cytosol and subcellular compartments such as inside lysosomal or mitochondrial spaces. It is unlikely that 2FDG-6P is contained within these subcellular organelles.

2FDG-6P, as a compartment-specific marker, offers many distinct advantages. First, the same molecule can be used *both* as an extra- and intracellular marker. This allows direct comparison of the motion within the extra- and intracellular spaces. Second, no MR signal suppression scheme is necessary because there is no tissue ^{19}F NMR background signal. Third, the large magnetogyric ratio of ^{19}F affords considerable signal-to-noise sensitivity and allows one to achieve b values close to those obtained with ^1H . Fourth, and most importantly, the plasma membrane is relatively impermeable to 2FDG-6P. In the time interval during which the diffusion measurement is sensitive to motion, the average 2FDG-6P molecule is very unlikely to cross the plasma membrane. This affords the compartment-specific ADC measurement *in the absence of transmembrane exchange*. Similar compartment-specific ADC measurements using the $^1\text{H}_2\text{O}$ signal are very difficult because compartment-specific signals for intra- and extracellular $^1\text{H}_2\text{O}$ cannot be readily distinguished, and transmembrane exchange of water may take place during the typical diffusion measurement.

Compartment-Specific ADC Values of 2FDG-6P

Restricted Diffusion

The 2FDG-6P ADC values in the two cellular compartments are statistically indistinguishable in either normal or globally ischemic rat brain. This implies that ADC values of water in both compartments are similar. The ADC values of intracellular 2FDG-6P *in vivo* reported here are similar to those found for other endogenous intracellular biomolecules of like size, such as N-acetylaspartate (NAA), creatine (Cr), and choline (Cho) (18, 19, 62, 64, 65). As of yet, there are no literature values for diffusion of small molecules in the extracellular space of brain with which to compare our values for extracellular 2FDG-6P (MW = 260 g/mole). We have made preliminary ADC measurements of extracellular mannitol

Table 2b
Rat Brain In Vivo Intracellular 2FDG-6P ADCs and Relaxation Time Constants at 4.7 T and 37°C (mean \pm SD, $n = 7$).

	T_1 (s)	T_2 (s)	ADC (10^{-3} mm 2 /s)
Alive	1.36 \pm 0.10	0.106 \pm 0.010	0.157 \pm 0.028
Dead	1.43 \pm 0.11	0.101 \pm 0.011	0.099 \pm 0.021 ^a

^a Average of all measurements after death.

(MW = 182 g/mole) by detecting the ^1H resonance at 3.7 ppm using PRESS volume-localized diffusion spectroscopy. Mannitol has been well described as a marker for the extracellular space (66, 67) and can be administered via intracerebroventricular infusion. Our data, obtained with a diffusion time of 20 ms, are quantitatively very similar to the results obtained with extracellular 2FDG-6P (data not shown).

These data do not suggest that the ADC value of 2FDG-6P in the relatively large volume of the cerebroventricular space (such as the lateral ventricles) is similar to that in the intracellular or interstitial space. Based on literature values (68), we estimate that the lateral and third ventricles together constitute only about 7% of total brain extracellular volume in rat. Further, with the use of surface coil localization, the third ventricle lies in a region of relatively low receiver coil sensitivity. Therefore, the MR signal from extracellular 2FDG-6P arose primarily from the interstitial space where diffusion may be highly restricted due to encounters with plasma membranes. Assuming that 2FDG-6P ADC values reflect water motion, the ADC values of water in the two compartments are likely to be similar in magnitude.

The widely held assumption that the water ADC value in the extracellular space is markedly greater than that in the intracellular space is open to question. The assumption is based on the notion that diffusion in the extracellular space is more rapid because the extracellular space contains a relatively low concentration of macromolecules, i.e., is more like pure water, as compared with the intracellular space. However, the average interstitial distance between plasma membranes in brain, as estimated via microscopy, is 10–30 nm (69, 70). These tightly-confining boundaries of the extracellular space might well be expected to reduce the ADC values for both extracellular 2FDG-6P and extracellular water due to restricted diffusion. It is important to note that this distance may be somewhat greater following administration of 2FDG-6P into the extracellular space because of osmotic effects that would tend to expand the extracellular space. We expect this effect to be minor because the concentration of extracellular 2FDG-6P used was ~ 2 mM.

Diffusion in the presence of barriers is commonly referred to as restricted and/or hindered diffusion. The likelihood of a molecule encountering a barrier in the time interval (t_{diff}) during which the diffusion measurement is sensitive to movement can be evaluated by calculating the root mean square displacement, $\langle x^2 \rangle^{1/2}$, for a molecule in the direction of the applied gradient

$$\langle x^2 \rangle^{1/2} = \sqrt{2 \text{ADC}(\Delta - \delta/3)} = \sqrt{2 \text{ADC} t_{\text{diff}}} \quad [3]$$

[Even though molecular motion is three-dimensional, the application of a given diffusion-gradient pulse sensitizes the experiment to molecular motion in one dimension. The root mean square displacement has been computed for one dimension; thus, the factor of $\sqrt{2}$ rather than $\sqrt{6}$.] For the diffusion time of 22.2 ms employed in this study, the root mean square displacement of a typical extracellular 2FDG-6P molecule is ~ 2.5 μm . Given the short distance between plasma membrane described above, the typical extracellular 2FDG-6P molecule would encounter

the plasma membrane many times during its ADC measurement. As a consequence, the ADC value of extracellular 2FDG-6P is likely to be reduced due to restricted diffusion. Water molecules, which have a higher ADC value, would be expected to have an even larger root mean square displacement. Unlike 2FDG-6P, water molecules may pass through the plasma membrane after some of their encounters with it, though the membranes would still hinder diffusion. Thus, the ADC values of molecules (including water) in the extracellular space are likely to be significantly reduced due to restricted diffusion and may be reduced to values similar to those found in the intracellular space.

With regard to the intracellular space, the average cell diameter in an adult rat brain is about 10 μm (19), though these cells have many processes, such as axons and dendrites, with significantly smaller diameters. The mean square displacement of intracellular 2FDG-6P for a diffusion time of 24.5 ms is $\sim 2.7 \mu\text{m}$. This makes it likely that some 2FDG-6P molecules do not encounter the plasma membrane during the ADC measurement, though their motion may be restricted by encounters with the membranes of intracellular organelles. Thus, the intracellular 2FDG-6P ADC values may also reflect some degree of restricted diffusion. Further, ADC values in the intracellular space may be reduced by its relatively high viscosity caused by a high concentration of macromolecules. Overall, these considerations do not significantly alter the major observations of this study—that the 2FDG-6P ADC values in both compartments are similar and decrease after global ischemia. Further, the diffusion times (and, hence, mean square displacements) used here are, if anything, shorter than those typically used in studies done on human subjects. As a result, restricted or hindered diffusion is likely to be a factor in the vast majority of clinical studies.

Biophysical Mechanisms of ADC Changes

The ADC value of intracellular 2FDG-6P decreases after cerebral ischemia. This decrease is consistent with that observed for intracellular $^{133}\text{Cs}^+$ (20) and endogenous intracellular metabolites (18, 19). Similarly, the ADC value of extracellular 2FDG-6P also decreases after cerebral ischemia. To our knowledge, this represents the first MR measurement of "extracellular" diffusion following brain injury.

The changes in the ADC of 2FDG-6P associated with cerebral ischemia can, in principle, be a consequence of changes in several factors, including (1) temperature, (2) transmembrane molecular exchange, (3) macroscopic bulk motion, (4) viscosity, (5) restrictive diffusion, (6) net movement of compartmental water, and (7) cytoplasmic motion. In this study, the rat brain temperature was carefully maintained at 37°C postmortem, and, thus, a change in temperature could not account for the 35–40% decrease in ADC values of 2FDG-6P.

With regard to transmembrane exchange, the plasma membrane is relatively impermeable to 2FDG-6P. As described above, the average 2FDG-6P molecule is unlikely to cross the plasma membrane in the time interval during which the diffusion measurement is sensitive to motion. Our observation of ADC decreases of extra- and intracellu-

lar 2FDG-6P in the absence of transmembrane exchange suggests that a change in membrane permeability, although still a possible consequence of cerebral ischemia, is not necessary to explain the decrease of water ADC value associated with cerebral ischemia. It has been suggested by others, using a red blood cell model, that a change in water permeability cannot entirely account for the observed ADC drop associated with cerebral ischemia (22). Similarly, it has been demonstrated with a theoretical tissue model and Monte Carlo simulation that ADC is relatively insensitive to changes in membrane water permeability (71).

The reduction in 2FDG-6P ADC associated with cerebral ischemia could be the result of a decrease of bulk motion on a macroscopic scale involving many cells. This postulate is prompted by the observation that ADC values of H_2O , NAA, Cr, Cho, and 2FDG-6P decrease about 30–45% as a result of various cell-injury models across different species. This observation suggests a common mechanism such as a reduction of brain macroscopic bulk motion associated with death. Such macroscopic bulk motion could be driven by or related to CSF pulsation and/or blood perfusion. We think this explanation is unlikely for two reasons. The first is that if this type of motion played a dominant role in molecular motion, then the ADC values for molecules in the brain, regardless of size, would be similar. This is clearly not the case, as the ADC value of $^1\text{H}_2\text{O}$ is roughly five times greater than the values of larger molecular-size metabolites. The second reason involves consideration of the ADC changes associated with brain injury. If significant bulk macroscopic motion were present, the ADC values for extremely slowly diffusing molecules would be dominated by this motion. The ADC values for more quickly diffusing species (e.g., $^1\text{H}_2\text{O}$) would be comprised of contributions from bulk motion as well as motion from other causes such as true "diffusion" or molecular transport. It is well documented that water ADC values decrease from a normal value of approximately $0.8 \times 10^{-3} \text{mm}^2/\text{s}$ in healthy rat brain to values of $\sim 40\%$ less after injury. This corresponds to a decrease in water ADC of $0.32 \times 10^{-3} \text{mm}^2/\text{s}$. If this decrease is due solely to changes in bulk macroscopic motion, then bulk macroscopic motion must cause molecular displacements corresponding to the ADC decrease of $0.32 \times 10^{-3} \text{mm}^2/\text{s}$. This motion would set the lower limit of ADC values for slowly diffusing metabolites in the brain to at least the value provided by bulk macroscopic motion. However, intracellular metabolites such as NAA have ADC values considerably less than this lower limit (often less than $0.2 \times 10^{-3} \text{mm}^2/\text{s}$). This indicates that, at least for water, bulk macroscopic motion makes at best a minor contribution to overall motion. Thus, bulk brain motion on a macroscopic scale is unlikely to be responsible for the ADC decrease associated with cerebral ischemia.

Another factor that may lead to the reduction of water ADC is an increase in cytoplasmic viscosity due to as yet unknown changes at a subcellular level associated with cerebral ischemia (19). The viscosity of water in the cytoplasm of healthy cultured cells has been estimated to be 1.2–1.4 (65, 72) or two to three times (73) that of bulk water. The apparent diffusion coefficient of intracellular 2FDG-6P in rat brain is considerably lower than that in

aqueous saline solution (Tables 1 and 2). This difference may reflect the combined effects of high cytoplasmic viscosity and hindrance of diffusion due to macromolecules in the cytoplasm and cell membrane barriers, such as endoplasmic reticulum. If cytoplasmic environment remains roughly the same after ischemia, the increase in cell volume due to the shift of water from the extra- to intracellular compartment associated with cellular edema would tend to decrease viscosity and thereby increase rather than decrease ADC values of intracellular metabolites (19). Thus, for this postulate to hold, intracellular viscosity must increase after cerebral ischemia despite an increase in intracellular water content. One possible mechanism by which this might occur is the dissociation of intracellular macromolecules, such as microtubules, after cell injury. However, it has been shown with fluorescence spectroscopy that disruption of the microtubules and microfilaments of the intracellular matrix with colchicine in human fibroblasts actually increases the ADC values of a microinjected intracellular marker threefold (74). A similar study using electron spin resonance also showed that the diffusion of spin-labeled molecules is increased by cytochalasin-induced microfilament disassembly in mouse fibroblasts (73). Therefore, it is unlikely that an increase in cytoplasmic viscosity due to the fragmentation of intracellular macromolecules is responsible for the water ADC decrease associated with cerebral ischemia. An increase in cytoplasmic viscosity due to other unknown mechanism(s) accompanying cell injury remains a possibility.

Another mechanism that may lead to a decrease in ADC values is an increase in the tortuosity of the space in which the molecule is contained. There is strong evidence that this occurs in the extracellular space. It has been proposed that cell swelling, which is associated with many forms of cell injury, presses cell membranes closer together in the extracellular space and thereby increases the tortuosity of this space. For example, van der Toorn *et al.* (24) infused tetramethylammonium (TMA^+) into the extracellular space of rat pup brain before and after ischemic injury. Diffusion curves for TMA^+ were measured using ion-selective electrodes and indicated a significant reduction in extracellular volume and an increase in extracellular tortuosity after ischemic brain injury. Based on their data, one can compute a 35% ADC decrease for TMA^+ associated with cerebral ischemia. This is consistent with the hypothesis that the 35–40% decrease in extracellular 2FDG-6P ADC value measured in the present study after global ischemia is due to an increase in tortuosity of the extracellular space. The increase in tortuosity would be expected to have a similar effect on the ADC of extracellular water, although, as mentioned above, water can pass through cell membranes. Nevertheless, a 35–40% decrease of extracellular ADC values *cannot* by itself completely account for the overall water ADC drop associated with cerebral ischemia. This is because the extracellular volume after cell swelling constitutes only ~10% of the total water brain signal. Given the findings of this study that the intra- and extracellular ADC values are statistically indistinguishable, a decrease in extracellular water ADC, even to a value of zero, for such a small volume fraction would account for only ~4% of the 30–45% decrease in weighted-average water ADC. This

would be true even in the presence of putative fast exchange between intra- and extracellular compartments.

It has been proposed that the water ADC decrease is due to the net migration of more rapidly diffusing extracellular water into the more slowly diffusing intracellular space as a result of cell swelling associated with cell injury (4, 5, 9, 12, 17). This hypothesis requires that diffusion in the extracellular space be sufficiently faster than in the intracellular space so that a <10% shift of total water could account for a ~40% overall water ADC decrease. Again, our data suggest that the water ADC values in the two compartments are likely to be very similar. Thus, such a shift of water would not significantly change the weighted-average water ADC value. As a result, we believe that a shift of water from the extra- to intracellular space is not a relevant mechanism by which water ADC values decrease after brain injury.

A final mechanism to be considered as a potential cause for the reduction in the ADC value of intracellular 2FDG-6P is cytoplasmic motion. It has been elegantly argued that an intracellular circulatory system is necessary for metabolic function in most cells and that simple diffusion cannot provide an explanation for intracellular transport at the molecular level (75–77). This motion perfuses the interior of the cell by streaming of the fluid compartment of the cytoplasm and is energy dependent. It has been postulated to take place in both labile and transient channels within the cell. Evidence for this motion includes the observation that fluorescent-tagged protein introduced into a HeLa cell by microinjection moves to all parts of the cell body (14–16 μm) within the time it takes to complete the injection, i.e., in approximately 1 s (76). If simple diffusion were the primary mechanism for this distribution, it would take about 26–27 min for the high molecular-weight fluorescent-tagged protein to distribute throughout the cytoplasm. Further, motion of cellular contents (both saltatory and streaming) can be directly observed in cells using laser Doppler and interference microscopy. This observed motion can be interrupted by moderate increase in cellular temperature and recovered by cooling after a short duration of high-temperature exposure (77). We suggest that cytoplasmic motion is present in brain cells, is energy dependent, and is interrupted by processes that cause cell injury and associated energy disruption or depletion. This leads to a reduction in the ADC values for molecules in the intracellular space, including both 2FDG-6P and water. This hypothesis is also consistent with data demonstrating a reduction of the ADC values for intracellular cesium (20) and intracellular metabolites (18, 19).

We propose that the loss of cytoplasmic circulation is very likely to be the predominant mechanism responsible for the decrease of intracellular and, thus, overall water ADC value (although an increase in cytoplasmic viscosity or restriction by means other than macromolecular dissociation remains a possibility and cannot be excluded based on the present study). The decrease in extracellular ADC value associated with cerebral ischemia is likely to make a relatively minor contribution to the overall water ADC change. Though water molecules, unlike 2FDG-6P molecules, are in exchange between these two compartments, the rapidity of this exchange (i.e., the average pre-exchange lifetime for a water

molecule in the intracellular space) has not yet been measured for brain cells. Nevertheless, whether this exchange takes place rapidly or slowly will not alter the major conclusions of this study.

Finally, we reiterate the underlying premise in this work, namely, that the motion of 2FDG-6P—as represented by the ADC measurement—may be taken to reflect the motion of the aqueous media comprising either the intra- or extracellular space. To the extent that this premise is accurate, one is able to draw inferential conclusions regarding compartment-specific water motion. However, should other factors, such as the binding or sequestration of 2FDG-6P to the macromolecular matrix, contribute significantly to the motional properties of 2FDG-6P, such inferential assessment is weakened. The use of other compartment-specific probes different from 2FDG-6P will, by comparison, allow the consistency of these findings to be evaluated and the possibility of inferential “artifact” to be assessed.

CONCLUSIONS

This study confirms the extra- and intracellular compartment specificity of 2FDG-6P *in vitro*. The extra- and intracellular ADCs of 2FDG-6P are statistically indistinguishable in normal as well as in globally ischemic rat brain and decrease 35–40% within 30 min after the onset of global cerebral ischemia. Assuming that 2FDG-6P ADC values reflect water motion in the two compartmental spaces, these results support the hypothesis that there are changes associated with cell injury that cause a reduction of water ADC values in *both* the extra- and intracellular compartments. They also suggest that the ADC values for water in the two spaces are similar. We propose that the predominant mechanism for the decrease in water ADC associated with cell injury is a reduction in the ADC value of intracellular water due to a decrease in energy-dependent intracellular circulation, although an increase in cytoplasmic viscosity or restriction by means other than macromolecular dissociation remains a possibility.

ACKNOWLEDGMENTS

The authors thank Dmitriy Yablonskiy for helpful discussion, Dennis W. Choi for use of his tissue culture facility, Andre' d'Avignon for assistance in obtaining $^{19}\text{F}\{^1\text{H}\}$ NMR spectra of the tissue culture samples, and G. Larry Bretthorst for help with Bayesian analysis.

REFERENCES

1. M. Brant-Zawadzki, B. Pereira, P. Weinstein, S. Moore, W. Kucharczyk, I. Berry, M. McNamara, N. Derugin, MR imaging of acute experimental ischemia in cats. *Am. J. Neuroradiol.* **7**, 7–11 (1986).
2. W. T. C. Yuh, M. R. Crain, D. J. Loes, G. M. Greene, T. J. Ryals, Y. Sato, MR imaging of cerebral ischemia: findings in the first 24 hours. *Am. J. Neuroradiol.* **12**, 621–629 (1991).
3. D. Davis, J. Ulatowski, S. Eleff, M. Izuta, S. Mori, D. Shungu, P. C. M. van Zijl, Rapid monitoring of changes in water diffusion coefficients during reversible ischemia in cat and rat brain. *Magn. Reson. Med.* **31**, 454–460 (1994).
4. M. E. Moseley, Y. Cohen, J. Mintorovitch, L. Chileuit, H. Shimizu, J. Kucharczyk, M. F. Wendland, P. R. Weinstein, Early detection of regional cerebral ischemia in cats: comparison of diffusion- and T_2 -weighted MRI and spectroscopy. *Magn. Reson. Med.* **14**, 330–346 (1990).
5. P. van Gelderen, M. H. M. de Vleeschouwer, D. DesPres, J. Parker,

- P. C. M. van Zijl, C. T. W. Moonen, Water diffusion and acute stroke. *Magn. Reson. Med.* **31**, 154–163 (1994).
6. J. C. Ford, D. B. Hackney, D. C. Alsop, H. Jara, P. M. Joseph, C. M. Hand, P. Black, MRI characterization of diffusion coefficients in a rat spinal cord injury model. *Magn. Reson. Med.* **31**, 488–494 (1994).
7. A. Righini, C. Pierpaolo, J. R. Alger, G. D. Chiro, Brain parenchyma apparent diffusion coefficient alterations associated with experimental complex partial status epilepticus. *Magn. Reson. Imaging* **12**, 865–871 (1994).
8. J. S. Park, T. Q. Duong, J. J. Neil, T. E. Conturo, J. J. A. Ackerman, Diffusion tensor imaging of the lithium/pilocarpine model of status epilepticus, in “Proc., ISMRM, 5th Annual Meeting, Vancouver, Canada, 1997,” p. 631.
9. J. Zhong, O. A. C. Petroff, J. W. Prichard, J. C. Gore, Changes in water diffusion and relaxation properties of rat cerebrum during status epilepticus. *Magn. Reson. Med.* **30**, 241–246 (1993).
10. J. Zhong, O. A. C. Petroff, J. W. Prichard, J. C. Gore, Barbiturate-reversible reduction of water diffusion coefficient in flurothyl-induced status epilepticus in rats. *Magn. Reson. Med.* **33**, 253–256 (1995).
11. H. B. Verheul, R. Balazs, J. W. B. van der Sprenkel, C. A. F. Tulleken, K. Nicolay, M. van Lookeren Campagne, Temporal evolution of NMDA-induced excitotoxicity in the neonatal rat brain measured with ^1H nuclear magnetic resonance imaging. *Brain Res.* **618**, 203–212 (1993).
12. H. Benveniste, L. W. Hedlund, G. A. Johnson, Mechanism of detection of acute cerebral ischemia in rats by diffusion-weighted magnetic resonance spectroscopy. *Stroke* **23**, 746–754 (1992).
13. K. Takano, L. L. Latour, J. E. Formato, R. A. D. Carano, K. G. Helmer, Y. Hasegawa, C. H. Sotak, M. Fisher, The role of spreading depression in focal ischemia evaluated by diffusion mapping. *Ann. Neurol.* **39**, 308–318 (1996).
14. L. L. Latour, Y. Hasegawa, J. E. Formato, M. Fisher, C. H. Sotak, Spreading waves of decreased diffusion coefficient after cortical stimulation in rat brain. *Magn. Reson. Med.* **32**, 189–198 (1994).
15. J. Rother, A. J. de Crespigny, H. D'Arceuil, M. E. Moseley, MR detection of cortical spreading depression immediately after focal ischemia in the rat. *J. Cereb. Blood Flow Metab.* **16**, 214–220 (1996).
16. Y. Hasegawa, L. L. Latour, J. E. Formato, C. H. Sotak, M. Fisher, Spreading waves of a reduced diffusion coefficient of water in normal and ischemic rat brain. *J. Cereb. Blood Flow Metab.* **15**, 179–187 (1995).
17. A. W. Anderson, J. Zhong, O. A. C. Petroff, A. Szafer, B. R. Ransom, J. W. Prichard, J. C. Gore, Effects of osmotically driven cell volume changes on diffusion-weighted imaging of the rat optic nerve. *Magn. Reson. Med.* **35**, 162–167 (1996).
18. A. van der Toorn, R. M. Dijkhuizen, C. A. F. Tulleken, K. Nicolay, Changes in metabolite diffusion induced by focal cerebral ischemia in rats. *Magn. Reson. Med.* **36**, 914–922 (1996).
19. M. Wick, Y. Nagatomo, F. Prielmeier, J. Frahm, Alteration of intracellular metabolite diffusion in rat brain *in vivo* during ischemia and reperfusion. *Stroke* **26**, 1930–1933 (1996).
20. J. J. Neil, T. Q. Duong, J. J. H. Ackerman, Evaluation of intracellular diffusion in rat brain via ^{133}Cs NMR. *Magn. Reson. Med.* **35**, 329–335 (1996).
21. E. Sykova, J. Svoboda, J. Polak, A. Chnata, Extracellular volume fraction and diffusion characteristics during progressive ischemia and terminal anoxia in the spinal cord of the rat. *J. Cereb. Blood Flow Metab.* **14**, 301–311 (1994).
22. L. L. Latour, K. Svoboda, P. P. Mitra, C. H. Sotak, Time-dependent diffusion of water in biological model system. *Proc. Natl. Acad. Sci. USA* **91**, 1229–1233 (1994).
23. D. G. Norris, T. Niendorf, D. Liebfritz, Healthy and infarcted brain tissue studies at short diffusion times: the origins of apparent restriction and the reduction in apparent diffusion coefficient. *NMR Biomed.* **7**, 304–310 (1994).
24. A. van der Toorn, E. D. R. M. Sykova, I. Vorisek, L. Vargova, E. Skobisova, M. van Lookeren Campagne, T. Reese, K. Nicolay, Dynamic changes in water ADC, energy metabolism, extracellular space volume, and tortuosity in neonatal rat brain during global ischemia. *Magn. Reson. Med.* **36**, 52–60 (1996).
25. J. A. Helpert, R. J. Ordidge, R. A. Knight, The effect of cell membrane permeability on the apparent diffusion coefficient of water, in “Proc., SMRM, 11th Annual Meeting, Berlin, Germany, 1992,” p. 1201.
26. B. M. Gallagher, J. S. Fowler, N. I. Guttererson, R. R. MacGregor, C.-N. Wan, A. P. Wolf, Metabolic trapping as a principle of radiopharma-

- ceutical design: some factors responsible for the biodistribution of [^{18}F]2-deoxy-2-fluoro-D-glucose. *J. Nucl. Med.* **19**, 1154–1161 (1978).
27. L. Sokoloff, M. Reivich, C. Kennedy, M. H. D. Rosiers, C. S. Patlak, K. D. Pettigrew, O. Sakurada, M. Shinohara, The [^{14}C]deoxyglucose method for the measurement of local cerebral glucose utilization: theory, procedure, and normal values in the conscious and anesthetized albino rat. *J. Neurochem.* **28**, 897–916 (1977).
 28. E. O. Stejskal, J. E. Tanner, Spin diffusion measurements: spin echoes in the presence of time-dependent field gradients. *J. Chem. Phys.* **42**, 288–292 (1965).
 29. R. L. Vold, J. S. Waugh, M. P. Klein, D. E. Phelps, Measurement of spin relaxation in complex systems. *J. Chem. Phys.* **48**, 3831–3832 (1968).
 30. D. E. Demco, P. V. Hecke, J. S. Waugh, Phase-shifted pulse sequence for measurement of spin-lattice relaxation in complex systems. *J. Magn. Reson.* **16**, 467–470 (1974).
 31. H. Y. Carr, E. M. Purcell, Effects of diffusion on free precession in nuclear magnetic resonance experiments. *Phys. Rev.* **94**, 630–638 (1954).
 32. E. L. Hahn, Spin echoes. *Phys. Rev.* **80**, 580 (1950).
 33. M. P. Goldberg, D. W. Choi, Combined oxygen and glucose deprivation in cortical cell culture: calcium-dependent and calcium-independent mechanisms of neuronal injury. *J. Neurosci.* **13**, 3510–3524 (1993).
 34. D. A. Kaku, M. P. Goldberg, D. W. Choi, Antagonism of non-NMDA receptors augments the neuroprotective effect of NMDA receptor blockade in cortical cultures subjected to prolonged deprivation of oxygen and glucose. *Brain Res.* **554**, 344–347 (1991).
 35. E. M. Bessel, P. Thomoas, The deoxyfluoro-D-glucopyranose-6-phosphates and their effect on yeast glucose phosphate isomerase. *Biochem. J.* **131**, 77–82 (1973).
 36. T. Nakada, I. L. Kwee, C. B. Conboy, Noninvasive *in vivo* demonstration of 2-fluoro-2-deoxy-D-glucose metabolism beyond the hexokinase reaction in rat brain by ^{19}F nuclear magnetic resonance spectroscopy. *J. Neurochem.* **46**, 198–201 (1986).
 37. B. A. Berkowitz, J. J. H. Ackerman, Proton decoupled fluorine nuclear magnetic resonance spectroscopy *in situ*. *Biophys. J.* **151**, 681–685 (1987).
 38. J. J. Kotyk, R. S. Rust, J. J. H. Ackerman, R. K. Deuel, Simultaneous *in vivo* monitoring of cerebral deoxyglucose and deoxyglucose-6-phosphate by ^{13}C [^1H] nuclear magnetic resonance spectroscopy. *J. Neurochem.* **53**, 1620–1628 (1989).
 39. T. Q. Duong, J. J. Neil, H. A. Stark, I. Palyka, C. S. Springer, S. Han, C. S. Sotak, J. J. H. Ackerman, Intracerebroventricular administration of compartment-specific NMR agents, in "Proc., ISMRM, 5th Annual Meeting, Vancouver, Canada, 1997," p. 1613.
 40. J. J. H. Ackerman, D. G. Gordon, G. K. Radda, G. G. Wong, Observation of ^1H NMR signals with receiver coils tuned for other nuclides. *J. Magn. Reson.* **42**, 498–500 (1981).
 41. C. T. Moonen, P. C. M. van Zijl, D. LeBihan, D. DesPres. *In vivo* NMR diffusion spectroscopy: ^{31}P applications to phosphorous metabolites in muscle. *Magn. Reson. Med.* **13**, 467–477 (1990).
 42. M. R. Patel, B. Siewert, S. Warach, R. R. Edelman, Diffusion and perfusion imaging techniques. *Magn. Reson. Imaging Clin. N. Am.* **3**, 425–438 (1995).
 43. K. D. Merboldt, D. Horstermann, W. Hanicke, H. Bruhn, J. Frahm, Molecular self-diffusion of intracellular metabolites in rat brain *in vivo* investigated by localized proton NMR diffusion spectroscopy. *Magn. Reson. Med.* **29**, 125–129 (1993).
 44. K. D. Merboldt, W. Hanicke, J. Frahm, Diffusion imaging using stimulated echoes. *Magn. Reson. Med.* **19**, 233–239 (1991).
 45. G. L. Bretthorst, "Bayesian Spectrum Analysis and Parameter Estimation," Vol. 48, Springer-Verlag, New York, 1988.
 46. G. L. Bretthorst, J. J. Kotyk, J. J. H. Ackerman, ^{31}P NMR Bayesian spectral analysis of rat brain *in vivo*. *Magn. Reson. Med.* **9**, 282–287 (1989).
 47. G. L. Bretthorst, Bayesian analysis. I. Parameter estimation using quadrature NMR models. *J. Magn. Reson.* **88**, 533–551 (1990).
 48. G. L. Bretthorst, Bayesian analysis. II. Model selection. *J. Magn. Reson.* **88**, 552–570 (1990).
 49. G. L. Bretthorst, Bayesian analysis. III. Applications to NMR signal detection, model selection, and parameter estimation. *J. Magn. Reson.* **88**, 571–595 (1990).
 50. C. Tanford, "Physical Chemistry of Macromolecules," John Wiley, New York, 1961.
 51. R. J. Melder, D. Elmaleh, A. N. Brownell, G. L. Brownell, R. K. Jain, A method for labeling cells for positron emission tomography (PET) studies. *J. Immunol. Methods* **175**, 79–87 (1994).
 52. F. Raggi, D. S. Kronfeld, M. Kleiber, Glucose-6-phosphatase activity in various sheep tissues. *Proc. Soc. Exp. Biol. Med.* **105**, 485–486 (1960).
 53. K. G. Prasannan, K. Subrahmanyam, Effect of insulin on the synthesis of glycogen in cerebral cortical slices of alloxan diabetic rats. *Endocrinology* **82**, 1–6 (1968).
 54. H. G. Hers, C. D. Duve, Le système hexose-phosphatase: repartition de l'activité glucose-6-phosphatase dans les tissus. *Bull. Soc. Chim. Biol.* **32**, 20–29 (1950).
 55. M. E. Phelps, S. C. Huang, E. J. Hoffman, C. S. Selin, L. Sokoloff, D. E. Kuhl, Tomographic measurement of local cerebral glucose metabolic rate in human with (^{18}F) 2-fluoro-2-deoxyglucose: validation of method. *Ann. Neurol.* **6**, 372–388 (1979).
 56. M. D. Revich, J. Kuhl, M. E. Greenburg, T. Phelps, V. Ido, J. Cassella, J. Fowler, A. Alavi, L. Sokoloff, The ^{18}F -fluorodeoxyglucose method for the measurement of local cerebral glucose utilization in man. *Circ. Res.* **44**, 127–137 (1979).
 57. A. Alavi, R. Dann, J. Chawluk, J. Alavi, M. Kushner, M. Reivich, Positron emission tomography imaging of regional cerebral glucose metabolism. *Semin. Nucl. Med.* **16**, 2–34 (1976).
 58. K. Wienhard, The FDG model and its application in clinical PET studies. *J. Neural Transm. Suppl.* **37**, 39–52 (1992).
 59. D. O. Slosman, N. Pittet, B. S. Polla, Fluorodeoxyglucose cell incorporation as an index of cell proliferation: evaluation of accuracy in cell culture. *Eur. J. Nucl. Med.* **20**, 1084–1088 (1993).
 60. P. Witkovsky, C.-Y. Yang, Uptake and localization of ^3H -2-deoxy-D-glucose by retinal photoreceptors. *J. Comp. Neurol.* **204**, 105–116 (1982).
 61. J. H. Simpson, H. Y. Carr, Diffusion and nuclear spin relaxation in water. *Phys. Rev.* **111**, 1201–1202 (1958).
 62. P. C. M. van Zijl, D. Davis, C. T. W. Moonen, Diffusion spectroscopy in living systems, in "NMR in Physiology and Biomedicine" (R. J. Gillies, Ed.), pp. 185–198, Academic Press, New York, 1994.
 63. B. Alberts, D. Bray, J. Lewis, M. Roff, K. Roberts, J. D. Watson, "Molecular Biology of the Cell," 2nd ed., Garland Publishing, Inc., New York, 1989.
 64. K. Yoshizaki, H. Watari, G. K. Radda, Role of phosphocreatine in energy transport in skeletal muscle of bullfrog studied by ^{31}P NMR. *Biochim. Biophys. Acta* **1051**, 144–150 (1990).
 65. M. J. Hubble, R. C. Rosanske, T. S. Moerland, Diffusion coefficients of ATP and creatine phosphate in isolated muscle: pulsed gradient ^{31}P NMR of small biological samples. *NMR Biomed.* **8**, 72–78 (1995).
 66. D. A. Brown, W. E. Stumpf, L. J. Roth, Location of radioactively labeled extracellular fluid indicators in nervous tissue by autoradiography. *J. Cell Sci.* **4**, 265–288 (1969).
 67. A. Van Harreveld, The extracellular space in the vertebrate central nervous system, in "The Structure and Function of Nervous Tissue" (G. H. Bourne, Ed.), Vol. 4, Academic Press, New York, 1972.
 68. C. E. Johanson, Ventricles and cerebrospinal fluid, in "Neuroscience in Medicine" (P. M. Conn, Ed.), pp. 171–196, J. B. Lippincott Company, Philadelphia, 1995.
 69. B. Cragg, Brain extracellular space fixed for electron microscopy. *Neurosci. Lett.* **15**, 301–306 (1979).
 70. R. L. Schultz, U. L. Karlsson, Brain extracellular space and membrane morphology variations with preparative procedures. *J. Cell Sci.* **10**, 181–195 (1972).
 71. A. Szafer, J. Zhong, J. C. Gore, Theoretical model for water diffusion in tissues. *Magn. Reson. Med.* **33**, 697–712 (1995).
 72. K. Fushimi, A. S. Verkman, Low viscosity in the aqueous domain of the cell cytoplasm measured by picosecond polarization microfluorimetry. *J. Cell Biol.* **112**, 719–725 (1991).
 73. A. M. Mastro, M. A. Babich, W. D. Taylor, A. D. Keith, Diffusion of a small molecule in the cytoplasm of mammalian cells. *Proc. Natl. Acad. Sci. USA* **81**, 3414–3418 (1984).
 74. J. W. Wojcieszyn, R. A. Schlegel, E.-S. Wu, K. A. Jacobson, Diffusion of injected macromolecules within the cytoplasm of living cells. *Proc. Nat. Acad. Sci. USA* **78**, 4407–4410 (1981).
 75. D. N. Wheatley, P. C. Malone, Heat conductance, diffusion theory, and intracellular metabolic regulation. *Biol. Cell* **79**, 1–5 (1993).
 76. D. N. Wheatley, Mini-review: on the possible importance of an intracellular circulation. *Life Sci.* **36**, 299–307 (1985).
 77. D. N. Wheatley, A. Redfern, R. P. C. Johnson, Heat-induced disturbances of intracellular movement and the consistency of the aqueous cytoplasm in HeLa S-3 cells: a laser Doppler and proton NMR study. *Physiol. Chem. Phys. Med. NMR* **23**, 199–216 (1991).